Vogel-Fulcher-Tammann freezing of a thermally fluctuating artificial spin ice probed by x-ray photon correlation spectroscopy

S. A. Morley, D. Alba Venero, J. M. Porro, S. T. Riley, A. Stein, P. Steadman, R. L. Stamps, S. Langridge, and C. H. Marrows

Phys. Rev. B **95**, 104422 — Published 16 March 2017

DOI: 10.1103/PhysRevB.95.104422

Vogel-Fulcher-Tammann Freezing of a Thermally Fluctuating Artificial Spin Ice Probed by X-ray Photon Correlation Spectroscopy

S. A. Morley,[1,*] D. Alba Venero,[2] J. M. Porro,[2] S. T. Riley,[3] A. Stein,[4]
P. Steadman,[5] R. L. Stamps,[6] S. Langridge,[2] and C. H. Marrows[1,†]

[1]*School of Physics and Astronomy,*
University of Leeds, Leeds LS2 9JT, United Kingdom
[2]*ISIS, STFC Rutherford Appleton Laboratory,*
Chilton, Didcot OX11 0QX, United Kingdom
[3]*School of Electronic and Electrical Engineering,*
University of Leeds, Leeds LS2 9JT, United Kingdom
[4]*Center for Functional Nanomaterials,*
Brookhaven National Laboratory, Upton, New York 11973, USA
[5]*Diamond Light Source, Chilton, Didcot OX11 0DE, United Kingdom*
[6]*SUPA, School of Physics and Astronomy,*
University of Glasgow, Glasgow G12 8QQ, United Kingdom

(Dated: February 23, 2017)

Abstract

We report on the crossover from the thermal to athermal regime of an artificial spin ice formed from a square array of magnetic islands whose lateral size, 30 nm $\times$ 70 nm, is small enough that they are dynamic at room temperature. We used resonant magnetic soft x-ray photon correlation spectroscopy (XPCS) as a method to observe the time-time correlations of the fluctuating magnetic configurations of spin ice during cooling, which are found to slow abruptly as a freezing temperature $T_0 = 178 \pm 5$ K is approached. This slowing is well-described by a Vogel-Fulcher-Tammann law, implying that the frozen state is glassy, with the freezing temperature being commensurate with the strength of magnetostatic interaction energies in the array. The activation temperature, $T_{\mathrm{A}} = 40 \pm 10$ K, is much less than that expected from a Stoner-Wohlfarth coherent rotation model. Zero-field-cooled/field-cooled magnetometry reveals a freeing up of fluctuations of states within islands above this temperature, caused by variation in the local anisotropy axes at the oxidised edges. This Vogel-Fulcher-Tammann behavior implies that the system enters a glassy state on freezing, which is unexpected for a system with a well-defined ground state.

PACS numbers: 75.40.Gb, 75.50.Tt, 75.75.Jn, 05.40.-a

INTRODUCTION

In the past decade a new species of magnetic metamaterials has emerged: the artificial spin ices (ASI) [1, 2]. They consist of a 2-dimensional array of nanoscale magnetic islands arranged so that the magnetostatic interactions between the islands are geometrically frustrated [3]. The size and shape of the individual islands are designed with the intention that their shape anisotropy means they act as single-domain Ising-like macrospins, mimicking the atomic spins of their naturally-occurring 3-dimensional analogs [4–6], but confined to a plane. They are thus close to being realizations of the square ice vertex models solved by Wu [7] and Lieb [8]–one difference being that our experimental systems also possess weak long-range interactions–in which the exact microstate of the statistical mechanical system can be inspected using advanced microscopy methods. Until very recently, all ASIs studied have been athermal–albeit showing an effective thermodynamics [9–12]–since the shape anisotropy energy barrier E_{A} that must be surmounted to flip the magnetic moment of any one island is orders of magnitude larger than the thermal energy $k_{\mathrm{B}}T$ that can be reached experimentally. Whilst convenient for imaging studies, these athermal, arrested systems lack ergodicity and so fail to explore phase space in the manner of a true statistical mechanical system to find thermally equilibrated configurations, and thus were never close to attaining their antiferromagnetic ground state, which possesses long-ranged order [13, 14].

However, there are recent reports of thermalized ASIs, made either by heating the sample close to the Curie point of the material from which the islands are fabricated in order to drive dynamics [15], whereupon the arrested state may be imaged upon cooling [16, 17], or by using a one-shot anneal process that occurs during fabrication [18]. Within the last year or two, studies have been carried out that have dynamically imaged real-time thermal fluctuations in artificial spin ice in the square [19, 20], kagomé [21, 22], and tetris ice geometries [23]. Nevertheless the nature of the crossover from a thermally fluctuating system to the arrested, less ergodic state has so far received little attention. Here we report on measurements of an ASI with islands of lateral size 30 nm $\times$ 70 nm [24], shown in Fig. 1. By studying the time-dependence of their soft x-ray magnetic speckle scattering patterns, the ASI is shown to be thermal at room temperature and to freeze into a fully arrested state below ~ 178 K. The fluctuation rate follows a Vogel-Fulcher-Tammann law on cooling, implying that the frozen state is glassy in nature. There are several reports of bulk spin ice also showing

a lack of long-range order and unusual freezing observed in $Dy_2Ti_2O_7$ [25, 26]. Snyder et al. [25] attributed this to a softening of the crystal field anisotropy. A qualitatively similar explanation could apply to our results, where there is also softening of the uniaxial anisotropy within our nanomagnets.

EXPERIMENT

The ASI that we studied was fabricated using electron beam lithography with a lattice constant of 240 nm, as shown in Fig. 1. A lift-off process was used, with 8 nm thick Permalloy ($Ni_{80}Fe_{20}$) evaporated through the resist mask to form the islands, followed by a 2 nm Al cap. The substrate was a Si wafer. The ASI array had a 2 mm $\times$ 2 mm area ($\approx$ 140 million islands in total). Soft x-ray photon correlation spectroscopy (XPCS) coherent scattering measurements were carried out at the I10 beamline at Diamond in order to measure the time-time correlations of the magnetic fluctuations in the ASI. The experiments were carried out using circularly polarized light at the Fe L_3 (707 eV) resonance. The scattered intensity from the ASI was recorded in the reflection geometry (illustrated in Fig. 2(a)) using a charge coupled device (CCD) camera, mounted at a fixed scattering angle $2\theta = 9.6^\circ$, 80 cm from the sample, which was kept at a temperature of 223 K in order to reduce dark noise. Each image arose from a 40 ms exposure and the images were separated by the 4 s readout time of the camera. The transverse coherence length of the beam was calculated to be 14.9 μm, and so a 10 μm diameter pinhole was mounted 23 cm in front of the sample. Airy rings were observed when the direct beam was imaged through the pinhole, shown in Fig. 2(b), confirming the coherence of the beam. The samples were mounted for measurement on a temperature-controlled stage in the absence of any applied magnetic field.

RESULTS AND DISCUSSION

Since our ASI array has a square unit cell, it produces a square pattern of diffraction spots. In Fig. 2, the centre of the diffracted speckle pattern corresponds to $Q_x = 0$ and the first order peaks either side correspond to $Q_x = \pm 2\pi/a$, where a is the ASI lattice constant. The calculated lattice spacing for the ASI measured from the position on the array detector and the geometry was 239 ± 2 nm, which agrees with that obtained from scanning electron

microscopy (SEM), 243±4 nm. In previous scattering experiments on square ASIs incoherent light has been used to determine the different sublattice contributions to the hysteresis measured on different orders of diffraction [27], to observe half order magnetic ground state peaks from as-grown samples [28], or to observe quasi-pinch-points in the diffuse scatter that are related to the presence of a magnetic Coulomb phase[29].

When coherent illumination is used then the diffraction spot decomposes into speckle, arising from the disorder in the illuminated region of the sample introducing different phase shifts into the scattered waves [30]: this speckle is visible in the detailed views of the diffraction spots shown at the top of Fig. 2(a). The crux of the XPCS technique is that dynamics in the magnetic configuration is reflected in changes in the details of the speckle pattern. This effect has long been used with light at visible wavelengths to study relaxation and aging phenomena in soft matter [31]. XPCS experiments utilising hard x-rays have been used to study charge density waves associated with antiferromagnetic domains in Cr [32], giving an indirect measurement of magnetic dynamics. Soft x-rays at the M_5 resonance of Ho revealed antiferromagnetic domain fluctuations in a thin film of that metal [33], whilst the jamming of spiral magnetic domains in a Y-Dy-Y trilayer was revealed in the stretched exponential correlations studied using soft X-rays at the Dy M_5 resonance [34]. There have also been speckle scattering studies at the Co L_3 resonance using small-angle X-ray scattering geometry to study the effects of disorder on the domain pattern of multilayer perpendicular Co/Pt films in response to a field [35].

As expected, measurements taken at an energy of 700 eV, an energy that is below the Fe L_3 resonance, showed no change beyond random noise fluctuations (see Supplementary Movie 1), since the ASI physical structure is static. On tuning to the L_3 resonance at 709 eV, magnetic sensitivity is achieved and the speckle reconfigures as time passes, since the magnetic state of the sample is reconfiguring under thermal activity (see Supplementary Movie 2). The XPCS measurements were carried out at different temperatures to drive the thermal fluctuations at different rates. In order to quantify the time-dependent behaviour, we calculated the intensity-intensity temporal autocorrelation function [31],

$$g_2(\mathbf{Q},\tau) = \frac{\langle I(\mathbf{Q},t')I(\mathbf{Q},t'+\tau)\rangle_{t'}}{\langle I(\mathbf{Q},t')^2\rangle_{t'}} = 1 + A\left|F(\mathbf{Q},\tau)\right|^2, \qquad (1)$$

where $I(\mathbf{Q},t')$ is the intensity at wave vector $\mathbf{Q}$ at a time t', τ is the time delay, and $\langle ... \rangle_{t'}$ indicates a time average. $F(\mathbf{Q},t')$ is the so-called intermediate scattering function, and A is

a measure of the degree of speckle contrast. The g_2 function was calculated for each pixel within the speckle pattern of the Bragg peak, and averaged over all such pixels to give the autocorrelation $g_2(\tau)$ at each temperature, shown normalized to an initial value in Fig. 3(a).

These $g_2(\tau)$ curves were fitted with a heterodyne model, since the experimental setup means that the fluctuating magnetic signal is mixed with a static signal that comes from the charge scattering from the array structure [36]. This forms the equivalent of a reference beam in the measurement, leading to the following modified form of the Kohlrausch-Williams-Watts [37, 38] intermediate scattering function [39]:

$$g_2(\tau) = 1 + A\cos(\omega\tau)\exp\left(-(\tau/t_{\mathrm{r}})^{\beta}\right) \tag{2}$$

where t_{r} is the characteristic relaxation time, β is a stretching exponent, and ω is an oscillation frequency associated with the heterodyne mixing [39, 40]. The value of ω was found to be in the range $\approx$ 0.001-0.002 rads^{-1}, corresponding to a time period, $2\pi/\omega$ = 3,140 - 15,700 s ($\approx$ 1-4 hrs), which correlates well with the total measurement time. The speckle contrast coefficient, A, was found to be in the range 0.02-0.05, which agrees with that found from the visibility of the Airy pattern [41]. The fitted value of β in all our measurements was 1.0 ± 0.1, indicating equilibrated behavior [32]. One might expect a stretching exponent more than 1 for frustrated or jammed dynamics [34] or in the case of collective freezing into an ordered state would decrease from 1 to $\beta = 1/3$ at the freezing temperature [42], however we saw no appreciable temperature dependence of the stretching exponent within the error of the fits, in the temperature window measured.

At room temperature the system fluctuates too quickly and the speckle appears blurred due to the insufficient time resolution of our CCD acquisition. The correlation function drops off more and more slowly with decreasing temperature, as can be seen from the initial slope and the drop-off in Fig. 3(a). The g_2 function is flat at 180 K, since the speckle is static, and therefore the relaxation time must be much longer than the time of measurement ($\approx$ 3 hrs) at that temperature, and so cannot be accurately determined. We did not observe any increase in intensity of the peaks upon cooling. When comparing the interaction energy of our sample to other island sizes and lattice spacings in the literature, we are also in a fairly weak coupling regime. These data are consistent with the system retaining its symmetry whilst arresting, just as a glass does.

For temperatures between 190 and 250 K, t_{r} lies in the experimentally accessible range be-

tween these two extremes, as plotted in Fig. 3b. The simplest thermal activation behavior in a collection of magnetic nanoparticles is the Arrhenius-type Néel-Brown (NB) law expected for a non-interacting superparamagnetic system, $t_\mathrm{r} = \tau_0 \exp(T_\mathrm{A}/T)$, where $T_\mathrm{A} = E_\mathrm{A}/k_\mathrm{B}$ is an activation temperature and τ_0 is an activation time. As can be seen in the figure, this cannot be fitted to the data at all well. Also plotted is a fit based on the dynamical scaling law describing the critical slowing down (CSD) of a system on approaching a phase transition, $t_\mathrm{r} = \tau_0 \left[(T/T_\mathrm{C}) - 1\right]^{-z\nu}$ [43], which we also found to fit poorly and with the rather unrealistic value of $z\nu = 20$ [44]. On the other hand, a Vogel-Fulcher-Tammann (VFT) law [45–47] captures the low temperature detail much more accurately: the data were fitted with the expression

$$t_\mathrm{r} = \tau_0 \exp\left(\frac{T_\mathrm{A}}{T - T_0}\right), \tag{3}$$

where T_0 is the freezing temperature. The fit yields $T_\mathrm{A} = 40 \pm 10$ K and $T_0 = 178 \pm 5$ K.

The defining feature of a VFT law is the freezing temperature T_0, below which interactions in the system prevent any relaxation or fluctuation. Whilst the VFT law has been found to fit many different types of data sets very well, such as spin glasses, molecular magnets, super-cooled organic liquids, metallic liquids, and glassy (bio)polymer systems [48–50], it is nevertheless an empirical law not based on any underlying microscopic picture. Models that attempt to provide a VFT-like temperature dependence include–among others–ones based on a time-dependent percolation process [50], or on the energy distribution of the depth of coupled traps [51].

In the spin glass theory of Shtrikman and Wohlfarth (S-W) [52], from which a VFT law is derived, the random exchange interactions between the positionally disordered spins are represented by an average exchange field. The magnetostatic interactions in our ASI are real magnetic fields, making the S-W theory a natural one to adapt to our system. In it, the freezing temperature T_0 is determined by the characteristic magnetostatic interaction energy $E_\mathrm{i} = k_\mathrm{B}\sqrt{T_0 T_\mathrm{A}}$. Inserting the experimental values of T_A and T_0 from the fit of the VFT law to the data in Fig. 3(b), we obtain $E_\mathrm{i}/k_\mathrm{B} \approx 87$ K.

To assess whether this is physically reasonable, we estimated the scale of the magnetostatic interaction energy E_dip in our ASI using the OOOMF simulation package[53] and comparing a pair of islands in a collinear configuration. Assuming the nominal island size and spacing and the bulk magnetization of Permalloy ($M_\mathrm{s} = 800$ kA/m) yields $E_\mathrm{dip}/k_\mathrm{B} = 379$ K, which overestimates the experimental value of E_i by about about a factor of 4. Part of the

overestimate may be due to the extrinsic effect of the reduction in effective M_s [20] or the island volume, V, [54] due to oxidation. An intrinsic contribution to the overestimate is the fact that the total interaction energy arises from the sum of the frustrated interactions from all the island's neighbors, which will vary in sign and magnitude and sum up to be less than that from a single neighbouring island. Nevertheless, the expected scale of the magnetostatic interaction energies in the system is consistent with the measured value of the VFT freezing temperature T_0.

Now we turn to a discussion of the activation temperature T_A. We can estimate the energy barrier ΔE for Stoner-Wohlfarth coherent rotation of a single island, again assuming the bulk magnetization of Permalloy, using $\Delta E = KV = \ln(f_0 t_m) k_B T_A$, with the shape anisotropy constant $K = \frac{1}{2}\mu_0 \Delta\mathcal{D} M^2$, and the difference in demagnetizing factor along the two relevant directions $\Delta\mathcal{D} \approx 0.1$ based on the island geometry [55]. Here the measurement time, t_m, is taken as two hours, a typical data acquisition period, and we assume a typical attempt frequency $f_0 = 10$ GHz [56]. This yields $T_A \approx 1500$ K. This is far larger than the fitted T_A of 40 K, ruling out this simple picture.

In order to seek other evidence of thermally-activated processes that might cast light on this large discrepancy, standard zero-field cooled (ZFC) and field-cooled (FC) protocols were carried out on the samples using SQUID-vibrating sample magnetometry. First, in order to measure the ZFC curve, the sample was heated to 395 K and a large negative saturating field applied and removed, at this temperature it is expected that the sample will thermally fluctuate and disorder once the field is removed. The sample was then cooled to 5 K without any applied field, it is expected that on approaching a characteristic temperature the fluctuations will begin to slow and, in the absence of a bias field, the macrospins will freeze and should populate all magnetic microstates equally resulting in a demagnetised, low moment state. Then, a probe field of a selected magnitude was applied and the magnetic moment was measured during heating, which is the lower curve in each measurement in Fig. 4. Second, for the FC curve, the sample was measured again during cooling back down but this time with the magnetic field applied and in this case all microstates should align with the field to create a polarised, high moment state. The maximum in the ZFC, close to where the curves bifurcate, is defined as the average blocking temperature, T_B, and marked with a black arrow. For example, the data with probe field $\mu_0 H = 50$ mT has $T_B(50\text{ mT}) = 200 \pm 10$ K. The blocking temperature systematically rises for smaller

probe fields, and exceeds our experimental limit of 400 K at 5 mT. This behavior can be extrapolated to the case of zero applied probe field, using $T_{\mathrm{B}} \propto H^{2/3}$ (based on Ref. 57), which gives $T_{\mathrm{B}}(0\ \mathrm{mT}) = 460 \pm 20$ K. This is about a factor of four lower than that expected from the sample parameters and nominal volume, as previously calculated $T_{\mathrm{A}} \approx 1500$ K. Whilst reduced magnetization or volume can explain some of this discrepancy, it seems clear once again that a pure coherent rotation mechanism is unlikely to be strictly followed.

Nevertheless, there is another feature in the magnetometry data: there is an initial increase in moment up to 40 K, marked with a grey arrow, visible in all the ZFC curves. This signifies a much lower energy scale for some magnetic relaxation process, one that is strikingly similar to the T_{A} found from the VFT fit. As previously shown by Ozatay et al. [58], the properties of Py can change below 40 K when native oxidation has occurred. They showed in elements of a similar size that such oxidation is likely around the unprotected edges and can have significant effects on the reversal properties, where they observed an upturn in coercivity below this temperature.

We performed the same measurement and have plotted the coercivity of our sample as a function of temperature in Fig. 5. The same characteristic features as those seen in Ref. 58 are present. The line in the figure is a fit to Sharrock's equation [59], which describes the temperature dependence expected for the dynamic coercivity of magnetic particles. Ozatay et al. showed that for conformally capped islands this feature disappears and the coercivity can be fit to Sharrock's equation for all temperatures, whereas here and for their Py particles with a native oxide around the edges there is a sharp departure from this at around 40 K. They attribute this to the modification of the local anisotropy which arises from the exchange coupling between the antiferromagnetic oxide edges and the ferromagnetic Py. This results in different local anisotropy axes which create pinning points for the magnetization, and allow non-uniform reversal modes to become energetically accessible. This allows the system to sample a distribution of metastable states only once a temperature of $T_{\mathrm{A}} = 40$ K is exceeded.

CONCLUSIONS

To summarize, on cooling an artificial spin ice we have observed a dramatic lengthening of the relaxation time as measured by magnetic XPCS. The system slows abruptly as it crosses over from thermal equilibration to an athermal, frozen state. This crossover can be described

by a Vogel-Fulcher-Tammann law, which is typically used to describe glassy systems. The VFT freezing temperature $T_0 \approx 178$ K can be accounted for by the magnetostatic interaction strength through Shtrikman-Wohlfarth theory. The activation temperature $T_A \approx 40$ K arising from a fit of this law implies a much lower energy barrier to reversal than is expected from a single-domain coherent rotation picture. The value of 40 K appears to be determined by the modification of the anisotropy from oxidation at the edges of the islands. Whilst this manuscript was under review, we became aware of another experiment on artificial square ice in which relaxation measurements were performed by conventional magnetometry that also revealed a VFT law [60], albeit finding a rather different value of β to us.

The glass-like freezing is unexpected and remarkable since the square ice system is crystalline and possesses a long-range ordered ground state, unlike a conventional spin glass. This raises the question of the true nature of the glassy state that our artificial spin ice freezes into. VFT law behavior in crystals of molecular magnets has been interpreted as arising from growth of spin clusters in a cluster glass picture [48], which could also be the case here. Interestingly, recent studies have found that low temperature features in the specific heat and neutron scattering of the pyrochlore spin ice $Dy_2Ti_2O_7$, can be modelled by including random disorder into the system, such as oxygen vacancies [61]. This random disorder acts to soften the Ising axis and destroy the long-range order of the system, which can be qualitatively similar to our ASI system. Also, VFT-like freezing behaviour has recently been observed in the same material [62], prompting speculation about this representing many-body localization of spins in a translationally-invariant quantum system [63–65]. However, this is unlikely to be the case here since the artificial systems of the type we have studied consist of classical macrospins, ruling out explicitly quantum behavior, implying that some other unusual glass state is obtained in artificial spin ices once ergodicity is broken.

This work was supported by the EPSRC (grant numbers EP/J021482/1, EP/I000933/1, and EP/L002922/1). Research carried out in part at the Center for Functional Nanomaterials, Brookhaven National Laboratory, which is supported by the U.S. Department of Energy, Office of Basic Energy Sciences, under Contract No. DE-AC02-98CH10886. We would like to thank Diamond Light Source for beamtine and S. S. Dhesi for the loan of the CCD camera.

* Email: S.A.Morley@leeds.ac.uk

† Email: C.H.Marrows@leeds.ac.uk

[1] C. Nisoli, R. Moessner, and P. Schiffer, "Colloquium: Artificial spin ice: Designing and imaging magnetic frustration," Rev. Mod. Phys. **85**, 1473 (2013).

[2] L. J. Heyderman and R. L. Stamps, "Artificial ferroic systems: novel functionality from structure, interactions and dynamics," J. Phys.: Cond. Matt. **25**, 363201 (2013).

[3] R. F. Wang, C. Nisoli, R. S. Freitas, J. Li, W. McConville, B. J. Cooley, M. S. Lund, N. Samarth, C. Leighton, V. H. Crespi, and P. Schiffer, "Artificial 'spin ice' in a geometrically frustrated lattice of nanoscale ferromagnetic islands," Nature (London) **439**, 303 (2006).

[4] S. T. Bramwell and M. J. P. Gingras, "Spin ice state in frustrated magnetic pyrochlore materials," Science **294**, 1495 (2001).

[5] A. P. Ramirez, A. Hayashi, R. J. Cava, R. Siddharthan, and B. S. Shastry, "Zero-point entropy in 'spin ice'," Nature (London) **399**, 333 (1999).

[6] C. Castelnovo, R. Moessner, and S. L. Sondhi, "Magnetic monopoles in spin ice," Nature (London) **451**, 42 (2008).

[7] F. Y. Wu, "Exactly soluble model of the ferroelectric phase transition in two dimensions," Phys. Rev. Lett. **18**, 605 (1967).

[8] E. H. Lieb, "Exact solution of the problem of the entropy of two-dimensional ice," Phys. Rev. Lett. **18**, 692 (1967).

[9] C. Nisoli, R. Wang, J. Li, W. F. McConville, P. E. Lammert, P. Schiffer, and V. H. Crespi, "Ground state lost but degeneracy found: The effective thermodynamics of artificial spin ice," Phys. Rev. Lett. **98**, 217203 (2007).

[10] C. Nisoli, J. Li, X. Ke, D. Garand, P. Schiffer, and V. H. Crespi, "Effective temperature in an interacting vertex system: Theory and experiment on artificial spin ice," Phys. Rev. Lett. **105**, 047205 (2010).

[11] P. E. Lammert, X. Ke, J. Li, C.Nisoli, D. M. Garand, V. H. Crespi, and P. Schiffer, "Direct entropy determination and application to artificial spin ice," Nature Phys. **6**, 786 (2010).

[12] J. P. Morgan, J. Akerman, A. Stein, C. Phatak, R. M. L. Evans, S. Langridge, and C. H. Marrows, "Real and effective thermal equilibrium in artificial square spin ices," Phys. Rev. B

87, 024405 (2013).

[13] G. Möller and R. Moessner, "Artificial square ice and related dipolar nanoarrays," Phys. Rev. Lett. **96**, 237202 (2006).

[14] R. G. Melko, B. C. den Hertog, and M. J. P. Gingras, "Long-range order at low temperatures in dipolar spin ice," Phys. Rev. Lett. **87**, 067203 (2001).

[15] V. Kapaklis, U. B. Arnalds, A. Harman-Clarke, E. Th. Papaioannou, M. Karimipour, P. Korelis, A. Taroni, P C. W. Holdsworth, S. T. Bramwell, and B. Hjörvarsson, "Melting artificial spin ice," New J. Phys. **14**, 035009 (2012).

[16] J. M. Porro, A. Bedoya-Pinto, A. Berger, and P. Vavassori, "Exploring thermally induced states in square artificial spin-ice arrays." New J. Phys. **15**, 055012 (2013).

[17] S. Zhang, I. Gilbert, C. Nisoli, G.-W. Chern, M. J. Erickson, L. O'Brien, C. Leighton, P. E. Lammert, V. H. Crespi, and P. Schiffer, "Crystallites of magnetic charges in artificial spin ice," Nature (London) **500**, 553 (2013).

[18] J. P. Morgan, A. Stein, S. Langridge, and C. H. Marrows, "Thermal ground-state ordering and elementary excitations in artificial magnetic square ice," Nature Phys. **7**, 75 (2011).

[19] A. Farhan, P. M. Derlet, A. Kleibert, A. Balan, R. V. Chopdekar, M. Wyss, J. Perron, A. Scholl, F. Nolting, and L. J. Heyderman, "Direct observation of thermal relaxation in artificial spin ice," Phys. Rev. Lett. **111**, 057204 (2013).

[20] V. Kapaklis, U. B. Arnalds, A. Farhan, R. V. Chopdekar, A. Balan, A. Scholl, L. J. Heyderman, and B. Hjörvarsson, "Thermal fluctuations in artificial spin ice," Nature Nanotech. **9**, 514 (2014).

[21] A. Farhan, P. M. Derlet, A. Kleibert, A. Balan, R. V. Chopdekar, M. Wyss, L. Anghinolfi, F. Nolting, and L. J. Heyderman, "Exploring hyper-cubic energy landscapes in thermally active finite artificial spin-ice systems," Nature Phys. **9**, 375 (2013).

[22] I. A. Chioar, B. Canals, D. Lacour, M. Hehn, B. Santos Burgos, T. O. Menteş, A. Locatelli, F. Montaigne, and N. Rougemaille, "Kinetic pathways to the magnetic charge crystal in artificial dipolar spin ice," Phys. Rev. B **90**, 220407 (2014).

[23] I. Gilbert, Y. Lao, I. Carrasquillo, L. OBrien, J. D. Watt, M. Manno, C. Leighton, A. Scholl, C. Nisoli, and P. Schiffer, "Emergent reduced dimensionality by vertex frustration in artificial spin ice," Nature Phys. **12**, 162 (2015).

[24] S. A. Morley, A. Stein, M. C. Rosamond, D. Alba Venero, A. Hrabec, P. M. Shepley, M.-Y.

Im, P. Fischer, M. T. Bryan, D. A. Allwood, P. Steadman, S. Langridge, and C. H. Marrows, "Temperature and magnetic-field driven dynamics in artificial magnetic square ice," Proc. SPIE **9551**, 95511Q (2015).

[25] J. Snyder, J. S. Slusky, R. J. Cava, and P. Schiffer, "How spin ice' freezes," Nature **413**, 48–51 (2001).

[26] K. Matsuhira, Y. Hinatsu, T. Sakakibara, B. D. Gaulin, J. N. Reimers, T. E. Mason, J. E. Greedan, Z. Tun, and M. J. P. Gingras, "Novel dynamical magnetic properties in the spin ice compound $Dy_2Ti_2O_7$," Journal of Physics: Condensed Matter **13**, L737–L746 (2001).

[27] J. P. Morgan, C. J. Kinane, T. R. Charlton, A. Stein, C. Sánchez-Hanke, D. A. Arena, S. Langridge, and C. H. Marrows, "Magnetic hysteresis of an artificial square ice studied by in-plane Bragg x-ray resonant magnetic scattering," AIP Advances **2**, 022163 (2012).

[28] J. Perron, L. Anghinolfi, B. Tudu, N. Jaouen, J.-M. Tonnerre, M. Sacchi, F. Nolting, J. Lüning, and L. J. Heyderman, "Extended reciprocal space observation of artificial spin ice with x-ray resonant magnetic scattering," Phys. Rev. B **88**, 214424 (2013).

[29] O. Sendetskyi, L. Anghinolfi, V. Scagnoli, G. Möller, N. Leo, A. Alberca, J. Kohlbrecher, J. Lüning, U. Staub, and L. J. Heyderman, "Magnetic diffuse scattering in artificial kagome spin ice," Phys. Rev. B **93**, 224413 (2016).

[30] M. Sutton, S. G. J. Mochrie, T. Greytak, S. E. Nagler, L. E. Berman, G. A. Held, and G. B. Stephenson, "Observation of speckle by diffraction with coherent x-rays," Nature (London) **352**, 608 (1991).

[31] L. Cipelletti, L. Ramos, S. Manley, E. Pitard, D. A. Weitz, E. E. Pashkovski, and M. Johansson, "Universal non-diffusive slow dynamics in aging soft matter," Faraday Discuss. **123**, 237 (2003).

[32] O. G. Shpyrko, E. D. Isaacs, J. M. Logan, Y. Feng, G. Aeppli, R. Jaramillo, H. C. Kim, T. F. Rosenbaum, P. Zschack, M. Sprung, S. Narayanan, and A. R. Sandy, "Direct measurement of antiferromagnetic domain fluctuations," Nature (London) **447**, 68 (2007).

[33] S. Konings, C. Schüßler-Langeheine, H. Ott, E. Weschke, E. Schierle, H. Zabel, and J. B. Goedkoop, "Magnetic domain fluctuations in an antiferromagnetic film observed with coherent resonant soft x-ray scattering," Phys. Rev. Lett. **106**, 077402 (2011).

[34] S.-W. Chen, H. Guo, K. A. Seu, K. Dumesnil, S. Roy, and S. K. Sinha, "Jamming behavior of domains in a spiral antiferromagnetic system," Phys. Rev. Lett. **110**, 217201 (2013).

[35] M. S. Pierce, C. R. Buechler, L. B. Sorensen, S. D. Kevan, E. A. Jagla, J. M. Deutsch, T. Mai, O. Narayan, J. E. Davies, K. Liu, G. T. Zimanyi, H. G. Katzgraber, O. Hellwig, E. E. Fullerton, P. Fischer, and J. B. Kortright, "Disorder-induced magnetic memory: Experiments and theories," Phys. Rev. B **75**, 144406 (2007).

[36] S. K. Sinha, Z. Jiang, and L. B. Lurio, "X-ray Photon Correlation Spectroscopy Studies of Surfaces and Thin Films," Adv. Mater. **26**, 7764–7785 (2014).

[37] R. Kohlrausch, "Theorie des elektrischen rückstandes in der leidner flasche," Ann. Phys. Chemie (Poggendorff) **91**, 179 (1854).

[38] G. Williams and D. C. Watts, "Non-symmetrical dielectric relaxation behavior arising from a simple empirical decay function," Trans. Faraday Soc. **66**, 80 (1970).

[39] W. H. de Jeu, A. Madsen, I. Sikharulidze, and S. Sprunt, "Heterodyne and homodyne detection in fluctuating smectic membranes by photon correlation spectroscopy at x-ray and visible wavelengths," Physica B **357**, 39 (2005).

[40] M. Sutton, "A review of X-ray intensity fluctuation spectroscopy," C. R. Physique **9**, 657 (2008).

[41] G. Beutier, A. Marty, F. Livet, G. van der Laan, S. Stanescu, and P. Bencok, "Soft x-ray coherent scattering: Instrument and methods at ESRF ID08," Rev. Sci. Inst. **78**, 093901 (2007).

[42] Andrew T. Ogielski, "Dynamics of three-dimensional ising spin glasses in thermal equilibrium," Phys. Rev. B **32**, 7384–7398 (1985).

[43] C. Djurberg, P. Svedlindh, P. Nordblad, M. F. Hansen, F. Bødker, and S. Mørup, "Dynamics of an interacting particle system: Evidence of critical slowing down," Phys. Rev. Lett. **79**, 5154–5157 (1997).

[44] K. Gunnarsson, P. Svedlindh, P. Nordblad, L. Lundgren, H. Aruga, and A. Ito, "Dynamics of an Ising Spin-Glass in the Vicinity of the Spin-Glass Temperature," Phys. Rev. Lett. **61**, 754–757 (1988).

[45] H. Vogel, "Das Temperatur-abhängigkeitsgesetz der Viskosität von Flüssigkeiten (The law of temperature dependence of the viscosity of fluids)," Phys. Z. **22**, 645 (1921).

[46] G. S. Fulcher, "Analysis of recent measurements of the viscosity of glasses," J. Am. Ceram. Soc. **8**, 339 (1925).

[47] G. Tammann and W. Hesse, "Die Abhängigkeit der Viscosität von der Temperatur bei un-

terkühlten flüssigkeiten (The dependence of viscosity on temperature for undercooled fluids)," Z. Anorg. Allg. Chem. **156**, 245 (1926).

[48] D. A. Pejaković, J. L. Manson, J. S. Miller, and A. J. Epstein, "Photoinduced magnetism, dynamics, and cluster glass behavior of a molecule-based magnet," Phys. Rev. Lett. **85**, 1994 (2000).

[49] C. A. Angell, "Formation of glasses from liquids and biopolymers," Science **267**, 1924 (1995).

[50] M Cyrot, "A possible origin for the Vogel-Fulcher law," Phys. Lett. A **83**, 275 (1981).

[51] J.-P. Bouchaud, A. Comtet, and C. Monthus, "On a dynamical model of glasses," Journal de Physique I France **5**, 1521 (1995).

[52] S. Shtrikman and E. P. Wohlfarth, "The theory of the Vogel-Fulcher law of spin glasses," Phys. Lett. A **85**, 467 (1981).

[53] M. J. Donahue and D. G. Porter, "OOMMF User's Guide, Version 1.0," Interagency Report NISTIR 6376, National Institute of Standards and Technology, Gaithersburg, MD (1999).

[54] B. L. Le, D. W. Rench, R. Misra, L. O'Brien, C. Leighton, N. Samarth, and P. Schiffer, "Effects of exchange bias on magnetotransport in permalloy kagome artificial spin ice," New J. Phys. **17**, 023047 (2015).

[55] J. A. Osborn, "Demagnetizing factors of the general ellipsoid," Phys. Rev. **67**, 351 (1945).

[56] C. P. Bean and J. D. Livingston, "Superparamagnetism," J. Appl. Phys. **30**, S120 (1959).

[57] M. El Hilo, K. O'Grady, and R. W. Chantrell, "Susceptibility phenomena in a fine particle system 2. Field-dependence of the peak," J. Magn. Magn. Mater. **114**, 307 (1992).

[58] O. Ozatay, P. G. Gowtham, K. W. Tan, J. C. Read, K. A. Mkhoyan, M. G. Thomas, G. D. Fuchs, P. M. Braganca, E. M. Ryan, K. V. Thadani, J. Silcox, D. C. Ralph, and R. A. Buhrman, "Sidewall oxide effects on spin-torque- and magnetic-field-induced reversal characteristics of thin-film nanomagnets." Nature Mater. **7**, 567 (2008).

[59] M. P. Sharrock, "Time dependence of switching fields in magnetic recording media (invited)," J. Appl. Phys. **76**, 6413 (1994).

[60] M. S. Andersson, S. D. Pappas, H. Stopfel, E. Östman, A. Stein, P. Nordblad, R. Mathieu, B. Hjörvarsson, and V. Kapaklis, "Thermally induced magnetic relaxation in square artificial spin ice," Scientific Reports **6**, 37097 (2016).

[61] P. Henelius, T. Lin, M. Enjalran, Z. Hao, J. G. Rau, J. Altosaar, F. Flicker, T. Yavors'kii, and M. J. P. Gingras, "Refrustration and competing orders in the prototypical $Dy_2Ti_2O_7$ spin

ice material," Phys. Rev. B **93**, 024402 (2016).

[62] E. R. Kassner, A. B. Eyvazova, B. Pichler, T. J. S. Munsie, H. A. Dabkowskac, G. M. Luke, and J. C. S. Davis, "Supercooled spin liquid state in the frustrated pyrochlore $Dy_2Ti_2O_7$," Proc. Nat. Acad. Sci. **112**, 8549 (2015).

[63] W. De Roeck and F. Huveneers, "Scenario for delocalization in translation-invariant systems," Phys. Rev. B **90**, 165137 (2014).

[64] N. Y. Yao, C. R. Laumann, J. I. Cirac, M. D. Lukin, and J. E. Moore, "Quasi many-body localization in translation invariant systems," (2014), arXiv:1410.7407 [cond-mat.dis-nn].

[65] M. Schiulaz, A. Silva, and M. Müller, "Dynamics in many-body localized quantum systems without disorder," Phys. Rev. B **91**, 184202 (2015).

FIGURES

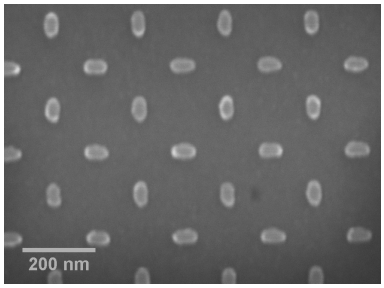

FIG. 1. Scanning electron micrograph of an artificial spin ice with a lattice spacing of 240 nm, with Permalloy islands of lateral size 30 nm × 70 nm and 8 nm thickness.

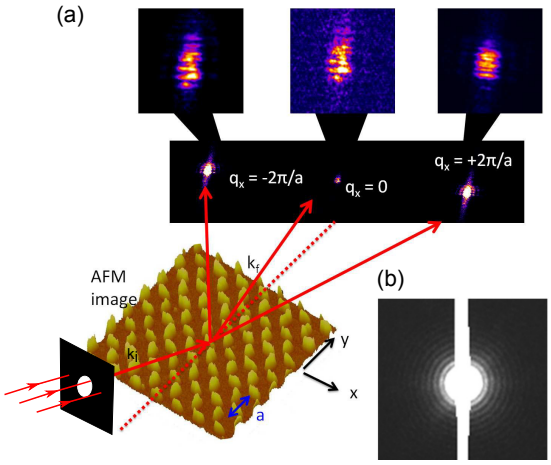

FIG. 2. (Color online) Coherent soft x-ray scattering measurements. (a) Schematic of the experimental XPCS setup, showing the incoming x-ray beam and scattered beams from the ASI array, which is represented by an atomic force microscopy image. The three main diffraction spots in the row above the specular reflection are shown here. Since the diffraction spots arise from a small, disordered region of the sample that has been coherently illuminated, they contain speckle contrast. (b) Fraunhofer diffraction obtained using the 10 μm pin hole and straight-through beam on to the CCD detector.

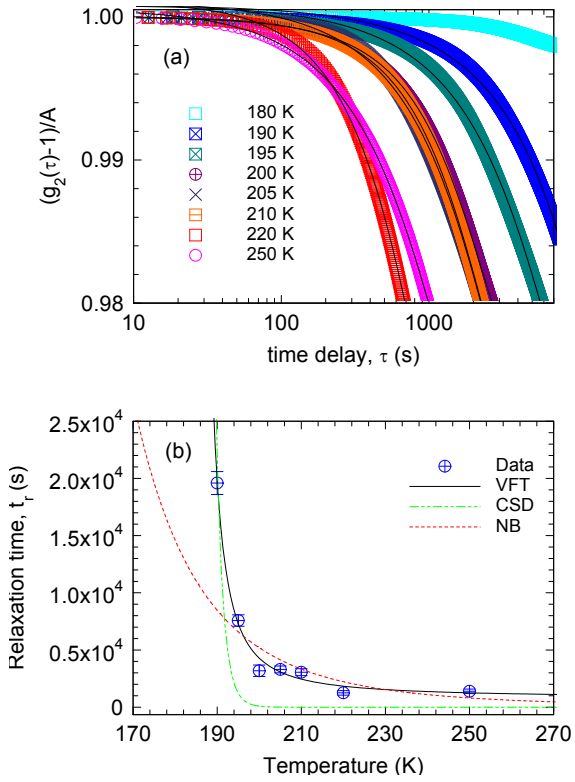

FIG. 3. (Color online) XPCS results. (a) Normalized $g_2(\tau)$ functions at various temperatures. The lines are fits to Eq. 2. (b) Relaxation times $t_{\rm r}$ as a function of temperature, fitted by a Vogel-Fulcher-Tammann (VFT) law. Also plotted is the superparamagnetic Néel-Brown (NB) law and critical slowing down (CSD) law near a phase transition, which fit poorly. Data points for $T = 180$ K (where $t_{\rm r} \gg 10^5$ s) and $T = 295$ K (where $t_{\rm r} \lesssim 5$ s) are not plotted since the experimental constraints mean that determining values within these bounds was not possible.

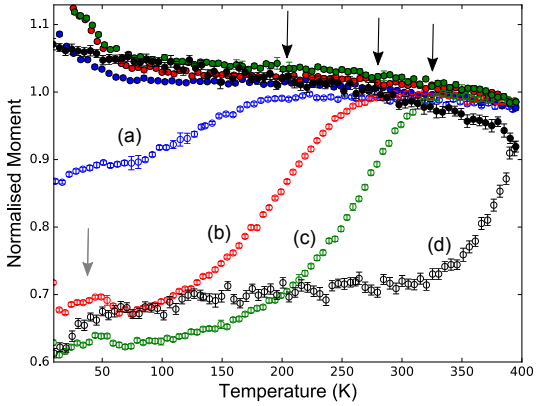

FIG. 4. (Color online) ZFC (open circles) and FC (filled circles) magnetization measurements under different applied magnetic probe fields of (a) 50 mT, (b) 35 mT, (c) 25 mT and (d) 5 mT. The average blocking temperature, T_B, is also defined by the maximum in the ZFC curve and is indicated by the black arrows ($T_B > 400$ K at 5 mT). The grey arrow indicates the ~ 40 K feature in the ZFC data. The field was applied along [01] direction of the ASI lattice.

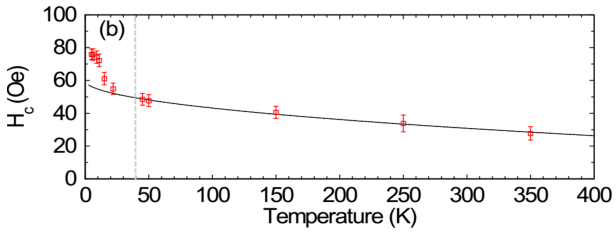

FIG. 5. (Color online) The temperature dependence of the coercivity measured along [01]. The line is a fit to Sharrocks equation, the departure from which is clear below 40 K (which has been indicated with the dotted line).